Magnetic Resonance Imaging 56 (2019) 37–44

Contents lists available at ScienceDirect

Magnetic Resonance Imaging

journal homepage: www.elsevier.com/locate/mri

Original Contribution

High temperature/pressure MAS-NMR for the study of dynamic processes in mixed phase systems

Ali Chamas[a,1], Long Qi[b,1], Hardeep S. Mehta[c], Jesse A. Sears[c], Susannah L. Scott[a,d], Eric D. Walter[c], David W. Hoyt[c,*]

[a] Department of Chemistry & Biochemistry, University of California, Santa Barbara, CA 93106, United States
[b] Ames Laboratory, U.S. Department of Energy, Ames, IA 50011, United States
[c] Environmental Molecular Sciences Laboratory, Pacific Northwest National Laboratory, Richland, WA 99354, United States
[d] Department of Chemical Engineering, University of California, Santa Barbara, CA 93106, United States

A B S T R A C T

A new MAS-NMR rotor (the *WHiMS* rotor) has been developed which can reach pressures of 400 bar at 20 °C or 225 bar at 250 °C. These rotors are ideal for mixed phase systems such as a reaction using a solid catalyst with a liquid/supercritical solvent topped with high pressure gas in the head space. After solid and liquid portions of the sample are loaded, the rotor is capped with an o-ring equipped polymer bushing that snaps into a mating groove in the rotor. The bushings incorporate a check valve into the sealing mechanism which allows for pressurization without mechanical manipulation – they will allow gas to flow in but not out. This *WHiMS* rotor design has enabled experiments on a wide variety of biotic and abiotic mixed-phase systems. Geochemical systems have also been studied, for example, adsorption and confinement studies of supercritical methane/CO_2 in clays and other minerals which display pressure dependent ^{13}C chemical shifts. Example data from other mixed-phase chemical and microbial systems are reported. These include monitoring metabolite conversion of extremophilic bacteria found in subsurface systems at elevated pressures and real-time *operando* reactions in catalysis systems - with liquid-quality resolution for ^{1}H and ^{13}C NMR spectra.

1. Introduction

In the last several decades great efforts have been devoted to the development of high temperature/pressure nuclear magnetic resonance (NMR) for *in situ* and *operando* studies [1,2]. Early efforts studying liquid and/or gas samples [3] have been achieved with Roe-style ceramic tubes (sapphire or zirconia) [4], capillary tubes [5], or polymer cells [6]. For solid or solid-containing samples, static mode was made possible by direct pressurization of the probehead or the sample cavity [7], which can be pressurized to as high as 25,000 bar [8]. Adoption of sealed Magic Angle Spinning (MAS) NMR began with use of a glass insert filled with the solid sample and pre-adsorbed gas or liquid before being sealed and transferred into a MAS NMR rotor [9]. More recently, apparatuses have been used to introduce gas molecules to rotors for *in situ* studies [10,11]. However, these MAS setups are incapable of introducing high pressure fluids or are intolerant of pressure build-up at higher temperature. Therefore, there is strong necessity to develop a sealed rotor design capable of handling elevated temperature/pressures and containing all phases of the analytes: a combination of solid, liquid and gas phase material. Simple o-ring seals on the rotor endcaps can provide a method of containing liquids and gases at near ambient pressure, and these products are offered by NMR instrumentation companies. Various lab-made designs have increased the pressure limits by trapping the o-ring beneath a screw; the internal threads that these screws engage are either in a bushing insert retained by adhesive in a commercial rotor, or integral to the ceramic of a custom machined monolith rotor [12].

Here, we discuss a new design, the *WHiMS* rotor (taken from the initials of the patent applicants – Walter, Hoyt, Mehta and Sears), that uses a mating ridge and groove to retain a bushing with integral o-rings in a commercial rotor. The addition of gas is facilitated by a modification of the o-ring grooves in the bushing, which allows them to work as a one-way check valve. This design can contain pressures in excess of 400 bar (depending on temperature, spinning rate and rotor size) and temperatures exceeding 250 °C [13]. Previous versions of this design have enabled *operando* spectra to be collected for growth of zeolite crystals or acid-catalyzed dehydration of cyclohexanol [14,15]. The latest design has a higher pressure/temperature range, which opens up the possibility of obtaining MAS-NMR spectra for much more challenging systems [16,17]. Our new results show the *WHiMS*-style MAS rotors are highly relevant for a wide range of temperature and pressure conditions, especially for *operando* studies of catalytic systems, with pressures possible to 200 bar at 250 °C [18,19]. Further, this *WHiMS*-style design allows for the utilization and observation of individual

* Corresponding author.
E-mail address: david.hoyt@pnnl.gov (D.W. Hoyt).
[1] Author contributions: A.C. and L.Q. contributed equally to this work.

https://doi.org/10.1016/j.mri.2018.09.026
Received 29 August 2018; Accepted 24 September 2018

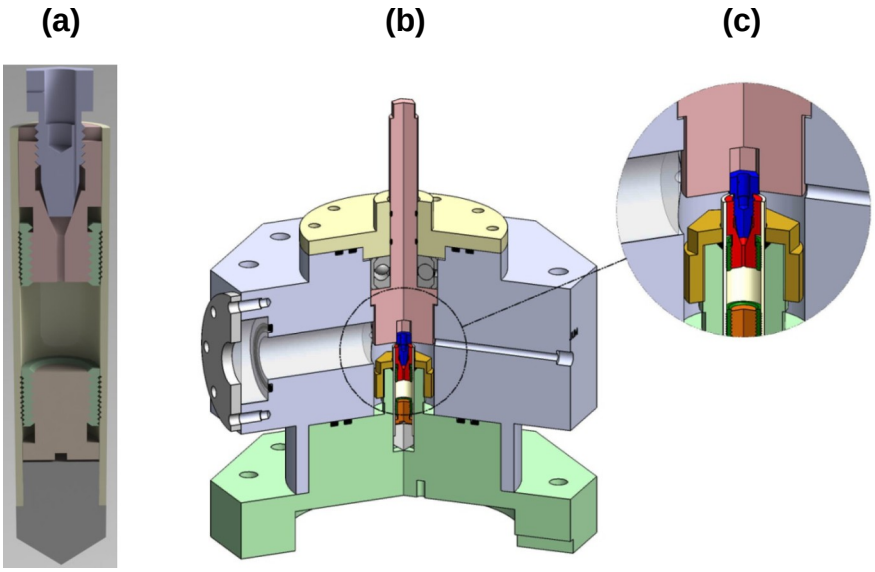

Scheme 1. The high-pressure PMAS rotor [27] and the rotor loading/reaction chamber. (a) Cross section of the assembled HP-MAS-R with the internal match/fit of the various components; (b) dissection view of the rotation mechanism for sealing the high-pressure rotor (top plate of the chamber); and the mechanism for tightly holding the rotor (bottom plate of the chamber); (c) a highlight of the mechanism used for *in situ* closing and opening the valve inside the high-pressure MAS rotor.

components of mixed phased systems (solid, liquid, gas, and/or supercritical fluids) simultaneously.

These recent advances in NMR have allowed for detailed structural and mechanistic information of multiphasic systems at elevated temperatures and pressures to be obtained [13,19]. Previously, the use of solid-state NMR in these multiphase systems had been limited due to the inability to reach both high temperatures and pressures [20,21]. We report findings using the new *WHiMS* style rotors in geochemistry and geoengineering looking at supercritical CO_2 intercalation and hydraulic fracturing fluid [16,22], biological systems probing the effects of sequestered CO_2 on microbial environments [23], and catalytic systems examining biomass valorization [13,17].

2. Design of *WHiMS* MAS rotors

Several pressurized MAS rotor systems [19,24] have been pioneered at PNNL, these were initially employed for geochemical [24–26] and biogeochemical [26] studies. Although these rotors were suitable for *in situ* MAS NMR examination of supercritical CO_2 containing systems, they required the use of a loading chamber that enabled mechanical opening and closing of the rotor valve under pressure, Scheme 1. The necessity of using a loading chamber resulted in time inefficiencies and an additional cost burden: a pressure vessel equipped with a mechanical feed-through is an expensive piece of custom equipment that requires increased consumption of gas (typically isotopically labeled) due to the dead volume. Furthermore, the high temperature adhesives used in the older rotors would degrade with steam or aggressive solvents above ~130 °C [19,24]. Although these rotors were generally useful up to 200 bar of pressure at temperatures to 100 °C, the temperature limitation imposed by the adhesive material prevented investigating many reactions of interest. A variation circumvented the use of adhesives by being constructed out of a ceramic monolith but had been limited to autogenic pressurization [12,15]. It was utilized to monitor a cyclohexanol based catalysis reaction up to ~150 °C and ~30 bar [20]. This design was similar to the early design, but other than the o-ring, is made entirely from ceramics. This rotor is ultimately limited in performance to that of the o-ring used as a seal, and in utility by the fact that gas cannot be added to the rotor; it relies on the increased vapor pressure of the solvent to build pressure.

WHiMS rotors are designed to allow *operando* studies of chemical reactions without compromising resolution or sensitivity. The rotors are a cavern style design, with one side permanently sealed by a ceramic end. To allow use on a wide range of equipment, standard rotor dimensions are used and the sealing device occupies the same space as a traditional end cap. Therefore, no hardware changes are required for use of these rotors on existing instruments. The standard rotor dimensions used also give the same sample space as standard NMR rotors (140 μL for 5 mm rotors and 400 μL for 7.5 mm style). This maximizes signal-to-noise as the sample space is not reduced by thicker rotor walls, extra ampoules, inserts, *etc*.

The *WHiMS* rotors are easily loaded with solid and liquid components and then sealed with a snap-in bushing and a hexagonal locking screw, Scheme 2. The bushing can slide in easily during insertion, due to the vertical slits in the bushing, and then locks into the machined groove in the sleeve. After snapping the bushing in place, a hexagonal locking screw is inserted to keep the bushing expanded and engaged with the machined groove. The ease of this process can be carried over into the glove box, where minimal tools are required to seal a sample in an air-free environment. After sealing, the rotor can be used as is or pressurized with gas without further exposing the sample to air.

Unlike previous designs [19,28], the *WHiMS* rotor uses a built-in one-way check valve for pressurization. The sealed rotor simply needs to be placed in a pressure vessel and exposed to the gas at the requisite pressure for the experiment. For experiments requiring an air-free environment, the rotor can be taken out of the glove box, placed in a pressure vessel and evacuated with a vacuum pump before pressurizing. Detailed control experiments probing the effect of the added gas can also be carried out using the *WHiMS* rotor design. This can be done by sealing the sample and initially running the experiment without the addition of gas, then upon completion of the experiment pressurizing the sample and running the experiment once more, all without the need to reopen the rotor. Furthermore, experiments requiring the presence of two or more gases (or a supercritical solvent and additional gas) can be carried out by sequential pressurizations.

The rotors have been bench-tested with N_2 gas at room temperature and shown to hold a pressure of 400 bar (6000 psi) for the 5 mm rotor size or 275 bar (4000 psi) for the 7.5 mm rotor. The rotors can use pressurization chamber of any style, with the simplest being a length of 3/8″ or 1/2″ tubing cut to the length of a rotor for a 5 mm or 7.5 mm rotor, respectively. The length of tubing can then be fitted with a cap on one end and reducer or union on the other, then attached to the regulator of a gas cylinder, which minimizes the dead volume of the system. Depressurization of the rotor is also made simple by inclusion of a pin hole in the bushing; simply loosening the hexagonal locking screw will allow for the safe release of pressure.

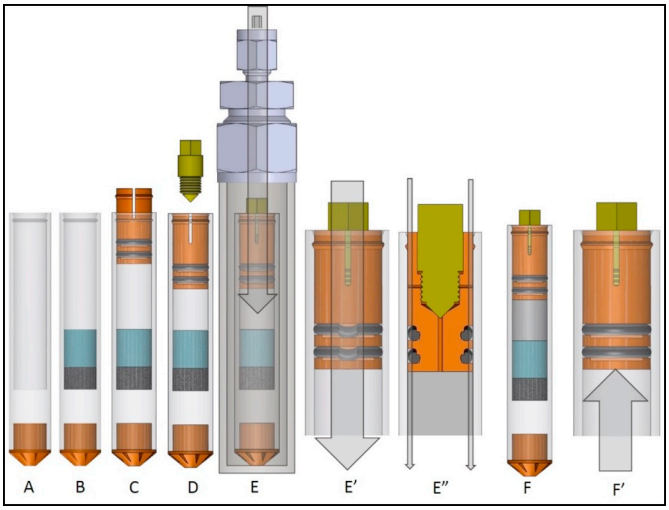

Scheme 2. Design of the high temperature/pressure *WHiMS* MAS rotors. A. Empty rotor; B. Rotor with solid and liquid samples added; C. Bushing installation; D. Locking screw installation, prevents gas escape through vent and retains bushing; E. Rotor in pressure vessel. E′. Close-up of check valve during pressurization. Gas (gray arrow) will flow into rotor and equalize with the pressure in the vessel by flexing the O-rings over cuts made into the O-ring grooves. E″. Close-up/cross-section view of check valve during pressurization. Rotor is shown rotated 90° from E′. Check valve cuts are placed 180° apart for balance resulting two paths for incoming gas (gray arrows). F. Pressurized rotor ready for NMR experiment with a three-phase reaction mixture, solid (black), liquid (blue) and gas (gray). F′. Close-up of check valve holding pressure with O-rings forced against unmodified side of the O-ring grooves by the internal pressure. (For interpretation of the references to colour in this figure legend, the reader is referred to the web version of this article.)
Reprinted with permission [13]. Copyright 2018, American Chemical Society.

3. Case study of dynamic processes in material research

The interface of materials with liquids and/or gases involves dynamic processes, which is crucial in the studies of geological processes, catalytic chemical production, *etc*. Such heterogeneous systems with dynamic processes have been poorly understood due to the difficulties of reaching high pressure and/or high temperature with non-perturbing tools. The *WHiMS* rotors are particularly applicable in these dynamic systems by offering a non-destructive measure for thermal or pressure-responsive processes. Table 1 is a list of broad-spectrum applications recently investigated by *WHiMS* rotors, with a wide range of temperature/pressure and a wide selection of unreactive and reactive liquids/gases.

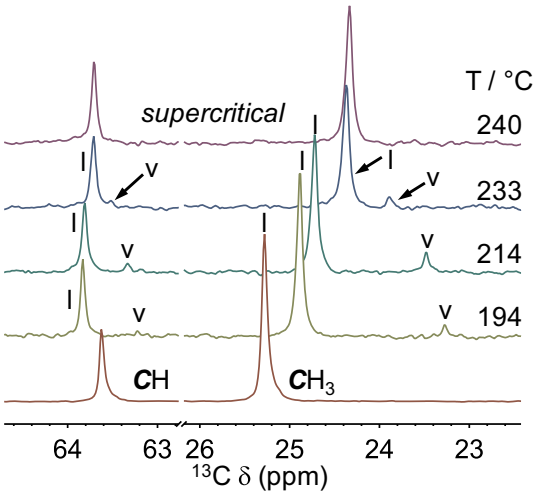

Fig. 1. Variable temperature ^{13}C MAS-NMR spectra of 2-PrOH (65 μL) in a sealed *WHiMS* rotor (5 mm). Each spectrum was acquired at a MAS rate of 3 kHz. Resonances corresponding to vapor and liquid species are denoted as v and l, respectively.
Adapted with permission [13]. Copyright 2018, American Chemical Society.

3.1. Monitoring phase transition

The supercritical point of 2-PrOH is 235.3 °C and 47 bar. In the ^{13}C NMR spectra, Fig. 1, the *WHiMS* rotor was loaded with 2-PrOH without pressurization from other gases; two new signals appeared at lower frequency relative to the methyl and methine resonances at temperatures above 150 °C. The appearance was fully reversible with these new peaks receding readily when the rotor is cooled. Therefore, the new signals were assigned to vapor-phase 2-PrOH. The intensity of the vapor phase peaks increased at higher temperature, while the intensities of the liquid-phase 2-PrOH signals decreased. At 240 °C, the vapor and liquid signals merged for both methyl (23.8 ppm) and methine (63.5 ppm) groups, consistent with the successful accomplishment of the supercritical state. In addition to supercritical 2-PrOH, the use of supercritical CO_2 as a solvent (shown below), as well as supercritical methane [29] and methanol have been identified in the *WHiMS* rotors.

Table 1
Dynamic systems studied with high temperature/pressure MAS NMR – *WHiMS* rotors.

	Systems	Liquid	Gas	Rotor (mm)	H Field (MHz)	Pressure (bar)	Temp °C[a]	Ref
1	Temperature calibration	Ethylene glycol		5	500	–	250	[13]
				7.5	300	–	225	
2	Geothermal fracturing	Water	Supercritical CO_2 or CH_4	5	500	90	50	[22]
		Water	CO_2	5	300	275	130	[16]
3	Lignin/model compound disassembly	2-PrOH[b]	H_2	5	500	213	250	[13]
		2-PrOH[b]	H_2	7.5	300	150	250	
4	Carbohydrate valorization	Water/GVL[c]		5	850	72	150	[17]
		Water/GVL[c]		7.5	500	72	150	
5	MOF[d]	THF[e]	H_2	5	500	80	220	[f]
6	Biomass pyrolysis	Pyrolysis oil	N_2 or H_2	7.5	300	138	180	[f]
7	Condensed-phase H_2	Methanol	CO_2 and H_2	5	600	160	325	[37]

[a] Temperature of sample as measured by lead nitrate standard; temperature of VT gas was 5–15 °C higher.
[b] 2-PrOH – 2-propanol.
[c] GVL – γ-valerolactone.
[d] MOF – Metal Organic Framework.
[e] THF – tetrahydrofuran.
[f] Unpublished results.

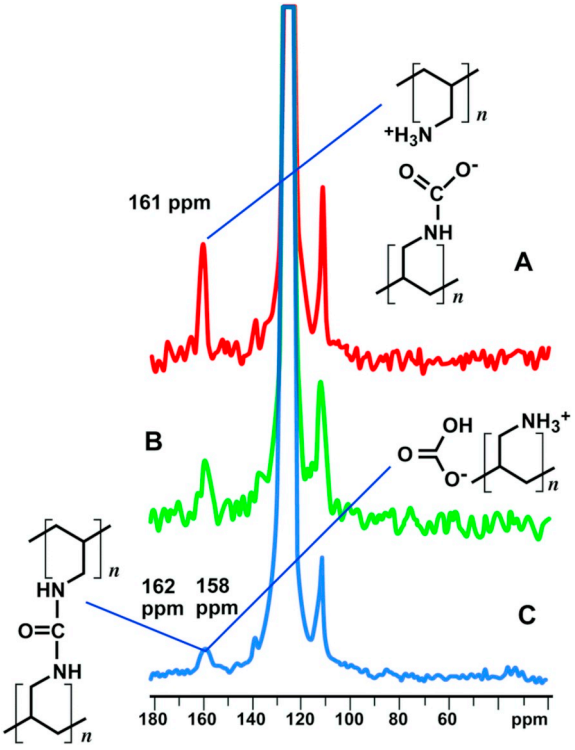

Fig. 2. ^{13}C MAS-NMR spectra of 1 wt% PAA solution exposed to 10% ^{13}C-labeled $scCO_2$ (A) at a temperature of 99 °C and a pressure of 103 bar, (B) at 127 °C and 121 bar, and (C) at 154 °C and 138 bar using a sample spinning rate of 1.0 kHz. These spectra were acquired with ^{1}H high power decoupling using a total of A) 120 scans, B) 120 scans, and C) 1000 scans respectively, with a recycle delay time of 5 s. The ^{13}C chemical shifts were referenced using an external reference, adamantane (37.85 ppm).
Reprinted with permission [16]. Copyright 2015, The Royal Society of Chemistry.

3.2. Geochemistry and geoengineering

Initially, the MAS rotor systems were employed for geochemical [24–26,30–34] and biogeochemical [23] studies. The use of *in situ* high temperature and pressure NMR rotors allowed for the examination of gel formation from hydraulic fracturing fluids under realistic pressures and temperatures. The rotors in this experiment were charged with an aqueous polyallylamine fracturing fluid (PAA) and supercritical CO_2 ($scCO_2$) in order to probe the speciation of CO_2 at varying temperatures. The single peak in Fig. 2a (99 °C) corresponds to the carbamate/carbamic acid species which decreases in intensity as a function of temperature. Upon reaching 154 °C Fig. 2c this signal transitions into two peaks at 158 and 162 ppm corresponding to PAA bicarbonate and cross-linked urea, respectively. The use of NMR in this study allowed for the speciation of the CO_2 species and viscosity determination. This system can undergo reversible volume expansions and the efficiency of this system is higher than conventional fracturing fluids [16].

A previous study looking at clay minerals (smectites) using *in situ* high-temperature and -pressure ^{13}C and ^{23}Na NMR, data showed that $scCO_2$ can effectively interact with the clay surfaces directly and also increase the site-hopping behavior of Na^+ with or without organic matter present. The presence of humic acids, the organic matter, resulted in a stronger CO_2 -surface interaction and that the CO_2 did not reacted to form an inorganic C-bearing species. This work helped demonstrate that the PMAS rotor system could be useful in understanding the fundamental binding, dynamics, and reactivity in these mineral-organo-H_2O-CO_2 systems [26].

Advances in the *in situ* rotors—particularly the implementation of a one-way check valve—allowed for pressurization without a specialized loading chamber. In the previous design, the rotor was placed in the loading chamber, pressurized, allowed to equilibrate, and then sealed. This procedure allowed any volatiles inside the rotor to exit during the equilibration step, preventing exact volatile-substrate ratios from being known. The one-way valve prevented drying of the sample by the supercritical fluid during the pressurization process. Bowers et al. compared the new rotor with the one-way check valve to the older "two-way" rotor in their paper looking at the role of cation in interactions of $scCO_2$ with clays at variable hydration, Fig. 3 [22]. The authors demonstrated that the properties of the charge-balancing cation can greatly change the CO_2 intercalation behavior. For instance, CO_2 intercalation was shown to be greater in clays containing cations of larger ionic radius and a smaller hydration energy, such as Cs-hectorite, compared with clays containing cations of high hydration energies and small ionic radii, *e.g.*, Na- and Ca-hectorite [22,34,35].

The authors complemented NMR experiments on Ca- and Cs-hectorite clays in the presence (red) and absence (black) of 90 bar $scCO_2$

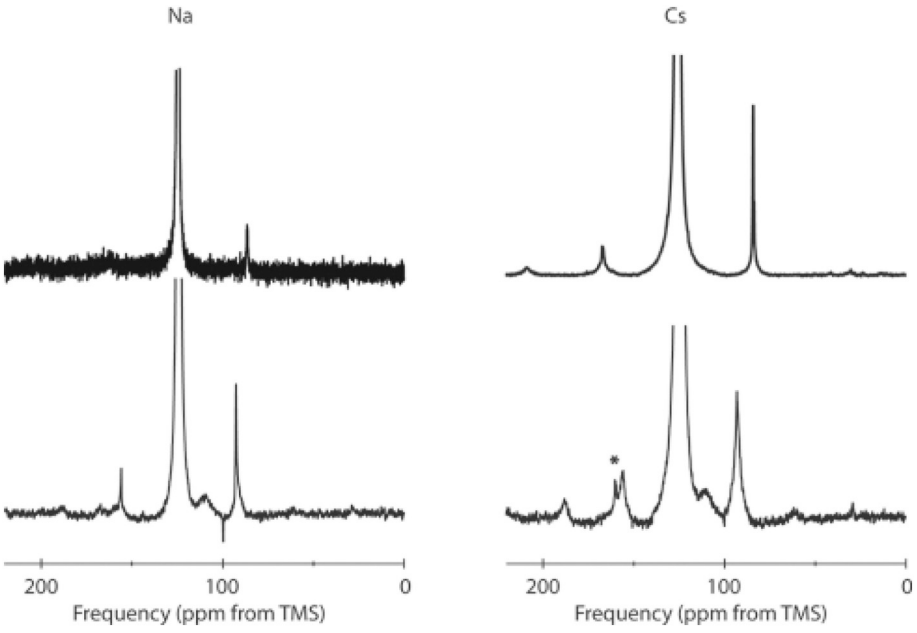

Fig. 3. Comparison of the ^{13}C MAS NMR spectra Na-hectorite and Cs-hectorite for samples initially equilibrated at 43% RH obtained with the two-way flow rotors (top row) and the one-way flow rotors (bottom row) acquired at 50 °C and 90 bar CO_2. Note that the SSB positions vary because of slightly different MAS spinning frequencies.
Reprinted with permission [22]. Copyright 2017, American Chemical Society.

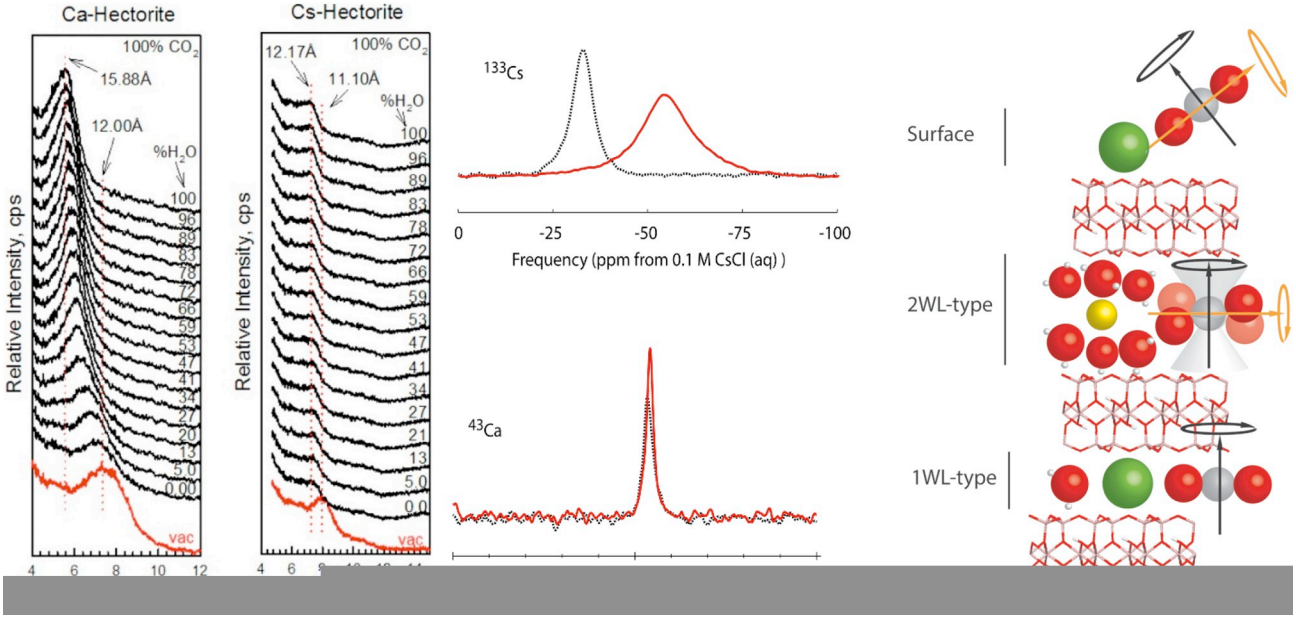

Fig. 4. X-ray diffraction (left) and NMR (center) data obtained for Ca- and Cs-hectorite obtained at 50 °C and 90 bar CO_2 as functions of the H_2O saturation of the $scCO_2$ phase. A graphical representation (right) shows the dominant orientations and rotational behavior of CO_2 molecules in different smectite structural environments. In 1WL-type interlayers (bottom right with green Cs^+) the CO_2 molecules lie dominantly parallel to the basal surfaces. In the 2WL-type interlayers (middle right) expected for example in fully hydrated Ca^{2+} (yellow)-saturated smectite, either CO_2 is absent, or it must be experiencing dynamics which on average has the same mean orientation and dynamically averaged line shape as in 1WL-type interlayers. On external surfaces (top panel) the orientation of the molecular rotation axis of the CO_2 can wobble and perhaps adopt a mean value that is not parallel to the basal clay surface while still undergoing rapid rotation about an axis perpendicular to the molecular long axis. (For interpretation of the references to colour in this figure legend, the reader is referred to the web version of this article.) Adapted with permission [22]. Copyright 2017, American Chemical Society.

with results from high pressure *in situ* x-ray diffraction (XRD), Fig. 4 and high pressure infrared spectroscopy (IR, data not shown). XRD tracks the spacing between the hectorite layers, while IR spectroscopy follows the amounts of H_2O and CO_2 sorbed to the clay. Increase in the interlayer spacing due to incorporation of CO_2 and/or H_2O is depicted by a decrease in the °2 Theta values from the basal reflection in X-ray diffraction data. Introduction of $scCO_2$ to the Cs-hectorite at 0% relative humidity leads to a significant expansion, indicative of CO_2 incorporation into the interlayer galleries, yet the basal spacing remains changes little with increasing levels of hydration. IR spectra show that CO_2 concentrations are at a maximum when the Cs-clay is fully dehydrated, but decrease with increasing relative humidity. These combined results indicate that H_2O outcompetes CO_2 for interlayer residency, while the basal layer spacing remains virtually unchanged. In contrast, the initially sub-1W Ca-hectorite shows less expansion upon the introduction of anhydrous CO_2, but the basal spacing increases with increasing relative humidity due to H_2O intercalation. Yet, similar to the Cs-clay, CO_2 concentrations are highest when the Ca-hectorite contains the least amount of interlayer H_2O, but decrease with increasing relative humidity and sorbed H_2O concentrations. These efforts demonstrate that by integrating results from not only *in situ* NMR but also IR and XRD, the authors provide a more complete description of the molecular-scale interactions between supercritical CO_2 and hectorite [22].

The effects of geological CO_2 sequestration on the microbial community were studied by Wilkins et al. [23] As previous reports have found active populations of sulfate-reducing bacteria (SRB) upon CO_2 injection [36], the model SRB (*Desulfovibrio vulgaris*) was used in this *in situ* NMR study to probe the metabolism of the bacteria at variable CO_2 pressures. The authors loaded the high-pressure NMR rotor with ^{13}C-labeled lactate and a washed cell suspension. After charging with 1 to 80 bar CO_2, the spectra were collected at 37 °C. At pressures of 1 and 5 bar CO_2 conversion of lactate to acetate was observed, Fig. 5. However, increasing the pressure to 10 bar or higher resulted in decreased conversion of the lactate and an increase in the fraction of dead cells. A complementary study carried out using 25 bar of N_2 showed no negative affect on the metabolism of lactate, indicating the decreased conversion at high pressures of CO_2 was not due to a pressure effect but likely the toxic effects of high CO_2 concentrations on the membrane integrity of the model SRB.

3.3. *Operando* heterogeneous catalysis

The *WHiMS* rotors allow the mixing of solids, such as catalytically active materials, with gases and liquids under MAS conditions. Thus, high-resolution NMR spectra can be acquired during the course of the reaction, which allows for the simultaneous detection of the reactants, products, intermediates, side-products, and solvents, with the potential to discriminate the phase or mobility of each species. Catalytic biomass conversion has been particularly challenging, typically requiring solid catalysts, solvents, and recalcitrant substrates. We have used the *WHiMS* rotors to carry out investigations on carbohydrates and lignin [13,17], the major components of biomass. In many cases, an isotopically labeled species was used in the reactant or solvent to enhance the desired signals and suppress the unwanted ones, minimizing acquisition time.

The glucose isomerization reaction can be catalyzed by solid base, such as NaX zeolite. Traditional methods can only provide information on the filtered reaction solution, but the reaction mostly occurs in the micropores of zeolite. We have mixed NaX zeolite in a 5 mm or 7.5 mm *WHiMS* rotor with glucose-1-^{13}C dissolved in aqueous solution of γ-valerolactone (GVL) (46 mol%), Fig. 6. The adsorption of glucose in the zeolite can be significantly improved by a GVL-water binary solvent without limitation of mass transfer in the catalytic reaction. At 25 °C, four resonances of glucose C1 can be detected. The two sharp signals can be assigned to the glucopyranose tautomers in the bulk solution and the two broad signals correspond to the adsorbed species inside the zeolite pores. The deconvolution of the quantitative ^{13}C NMR spectrum agrees with traditional adsorption studies, showing 65% of glucose

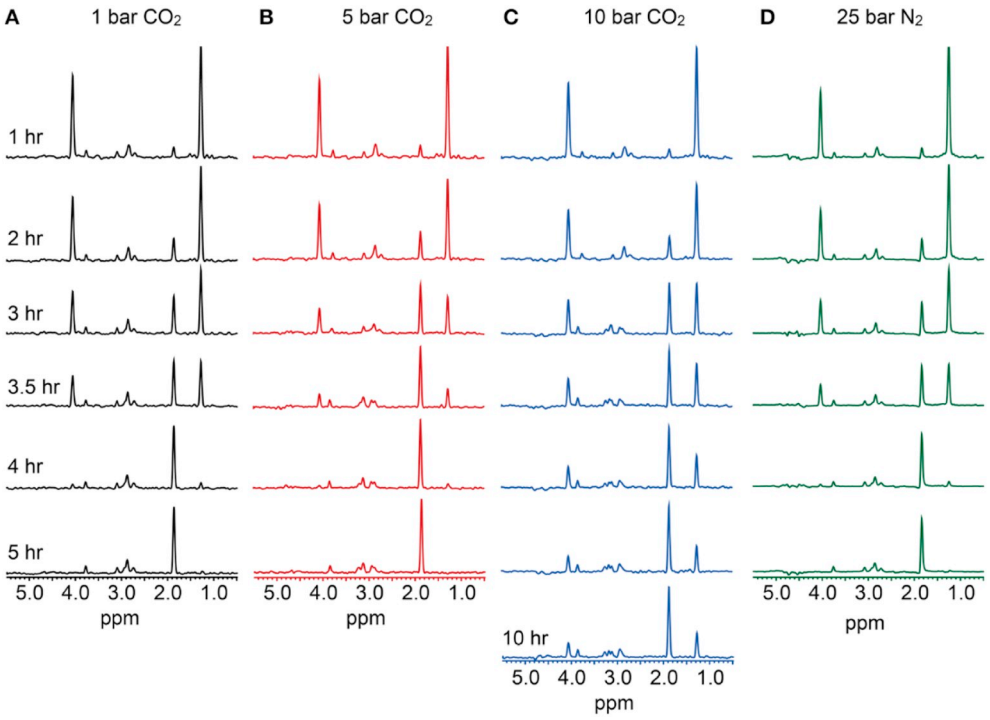

Fig. 5. *In situ* ^{13}C-filtered ^{1}H NMR data tracking microbial metabolism of ^{13}C-3-lactate to ^{13}C-2-acetate. The oxidation was monitored *via* the disappearance of lactate peaks at 4.04 and 1.26 ppm, which represent the lactate C—H and C—H_3 bonds, respectively. Concurrent to this, the peak appearing at 1.84 ppm represents the acetate CH_3 bond. Data indicates that at 1 bar CO_2 (A), 5 bar CO_2 (B), and 25 bar N_2 (D), complete conversion of lactate to acetate occurs over a 4–5 h. period. At 10 bar CO_2 (C) however, incomplete lactate oxidation is observed, supporting observations made in high-pressure CO_2 batch experiments.
Reprinted with permission [23]. Copyright 2014, Frontiers in Microbiology.

being adsorbed.

Upon temperature elevation to 120 °C, the signals of the adsorbed glucose sharpen as the mobility of the molecules is enhanced at higher temperature. In addition, all four glucose resonances start to decrease in intensity, due to the isomerization to fructose. The ratios among the adsorbed and mobile species stay unchanged during the course of the reaction, indicating the diffusion of glucose in-and-out of the zeolite is unlimited. Curve-fitting of the concentration profiles of glucose and

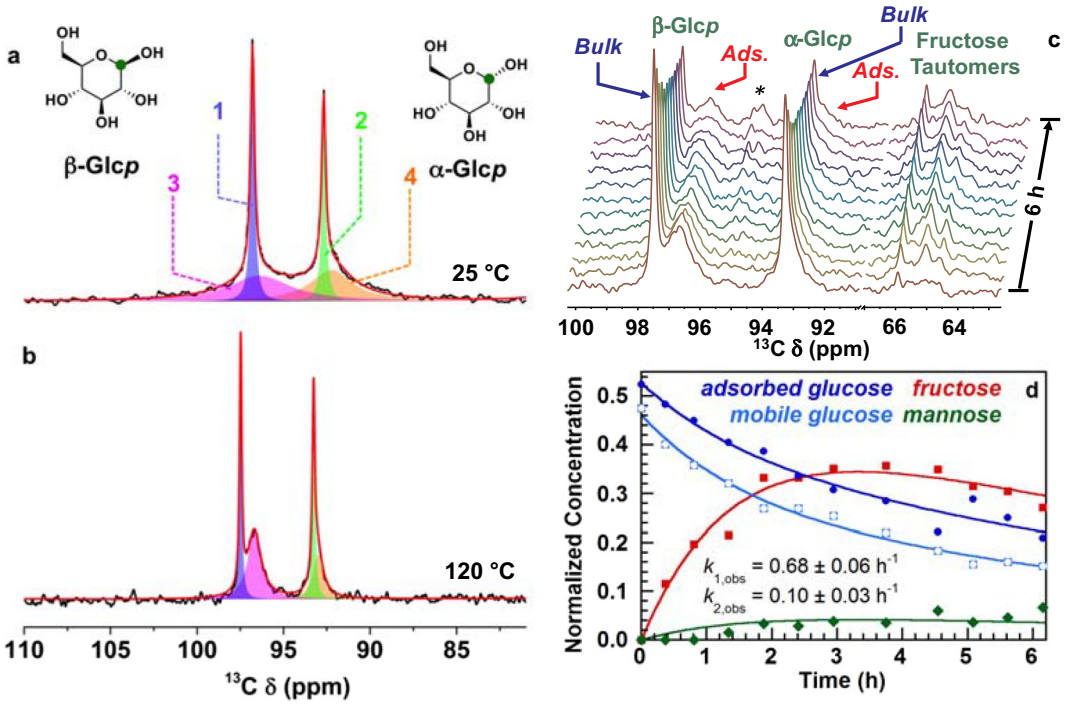

Fig. 6. Direct polarization MAS solid-state ^{13}C NMR study (125.77 MHz, 5 kHz MAS) of a mixture of NaX zeolite (200 mg) with a solution of glucose-1-^{13}C (0.100 mol L^{-1}, 1.00 mL) in 46 mol% of GVL at 25 and 120 °C: (a) spectrum recorded at 25 °C (green dots indicate the locations of the ^{13}C labels, corresponding to the observed signals); (b) first spectrum recorded shortly after heating the rotor to 120 °C. (c) Relative amounts of α-Glc*p* and β-Glc*p* glucose tautomers in the adsorbed or solution phases, as determined by solid-state NMR at 25 and 120 °C. (c) Time-resolved *operando* spectra, showing glucose conversion to fructose (* denotes mannose side-product). (b) Kinetic profiles (points) for glucose adsorbed in the zeolite, glucose present in the solution phase, total fructose, and total mannose. The lines are curve fits to a bi-exponential rate, where $k_{1,obs}$ and $k_{2,obs}$ are the pseudo-first-order rate constants for fructose production and degradation, respectively. (For interpretation of the references to colour in this figure legend, the reader is referred to the web version of this article.)
Adapted with permission [17]. Copyright 2017, American Chemical Society.

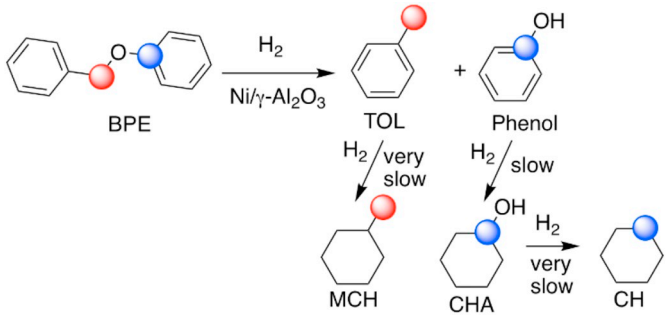

Scheme 3. Reaction mechanism for the Ni/γ-Al_2O_3 catalyzed hydrogenolysis of ^{13}C-labeled BPE, ((phenoxy-^{13}C)-methyl-^{13}C) benzene, at 225 °C with 120 bar H_2. The ^{13}C-labels are shown in red and blue circles for the methylene and phenolate ^{13}C resonances in BPE (labeled as BPE-B and BPE-P), respectively. (For interpretation of the references to colour in this figure legend, the reader is referred to the web version of this article.)

fructose reveals that both the isomerization and the further deactivation of glucose and fructose follow pseudo-first-order kinetics. The rate constant of the isomerization coincides well with the value obtained from a plug-flow reactor.

Unlike the isomerization of carbohydrates, the reductive disassembly of lignin usually demands high-pressure H_2 and a metal-based catalyst. To study the reaction mechanism and kinetics in lignin conversion, we investigated the hydrogenolysis of benzylphenylether (BPE) as a lignin α-O-4 model compound, with the rotor pressurized to upwards of 120 bar H_2. The BPE was ^{13}C labeled in both methylene and phenolate positions, Scheme 3, to keep track of changes to both products after cleavage of the ether linkage.

Operando NMR spectra were recorded during the catalytic hydrogenolysis of ^{13}C-labeled BPE at variable temperature, Fig. 7. The rotor was held at each temperature for 0.5 h before further heating to the next temperature setpoint, Fig. 7. After reaching 225 °C, the reaction was held at this temperature for 14 h. During the course of the non-isothermal portion of the experiment, the BPE signals gradually disappeared with the concurrent formation of those for toluene and phenol. Such transition is observed more readily in the ^{13}C MAS NMR spectrum, Fig. 7a. At 25 °C, the ^{13}C resonances of the methylene and phenolate-C^1 carbons of BPE are visible at 70.1 and 159.3 ppm, respectively. In the ^{1}H spectrum recorded, the methylene signals appear as a doublet at 4.9 ppm while the aromatic protons appear at 6.8–7.3 ppm, beside the H_2 resonance at 4.3 ppm, Fig. 7b. The conversion of BPE to toluene-α-^{13}C (20.8 ppm) and phenol-1-^{13}C (157.8 ppm) commences at 150 °C. After the complete conversion of BPE, at 200 °C, further hydrogenation of toluene and phenol was observed, with the slow formation of methylcyclohexane (MCH) and cyclohexanol (CHA), respectively. Furthermore, cyclohexane also showed up in the ^{13}C spectra after 14 h at 225 °C, from the hydrogenolysis of CHA. At elevated temperatures, signals for solvent 2-PrOH, phenol, toluene, and CHA in vapor phase are observed in both ^{13}C and ^{1}H MAS NMR spectra. A detailed kinetic study is currently under further investigation.

4. Conclusion

Recent advances in high temperature/pressure MAS rotor design, namely the *WHiMS* rotor, have allowed for a variety of *in situ* and *operando* studies on mixed phase systems. This includes not only solids, liquids and gases, but also supercritical fluids such as carbon dioxide, methane, isopropanol, and methanol, with simultaneous observation of these multiple phases being possible. Due to the one-way check valve in the *WHiMS* rotors, air-sensitive samples can be easily sealed in a glove box, allowing for sequential additions of multiple gases to be accomplished, resulting in complex mixtures of gases in the rotor without previous external mixing. This affords the ability to examine control samples by NMR before final catalytic conditions are achieved, without reopening the sealed rotor in *operando* NMR experiments. The range of conditions have been expanded to include temperatures as high as 325 °C and pressures to 400 bar, with a combined 200 °C/200 bar now a routine experiment. This capability has enabled the study of systems spanning geochemistry, catalysis, materials and microbiology, with new applications continually being added.

Acknowledgements

A.C., L.Q., and S.L.S. acknowledge funding from the U.S. National Science Foundation (CBET-1512228 and CBET-1604095). A.C. thanks UC Santa Barbara's Mellichamp Academic Initiative in Sustainability for

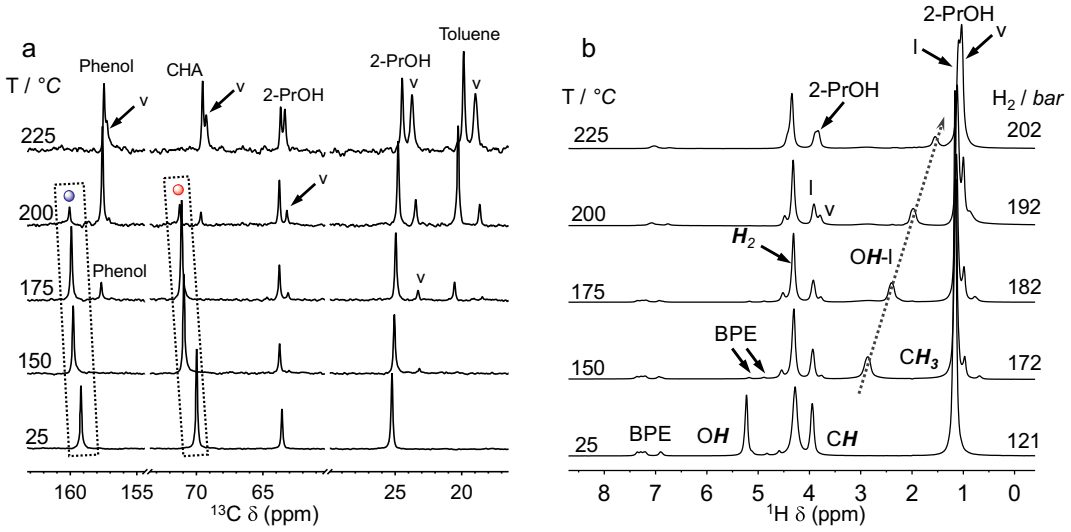

Fig. 7. Variable temperature (a) ^{13}C and (b) ^{1}H MAS NMR spectra of BPE hydrogenolysis carried out in 2-PrOH. The *WHiMS* rotor was charged with ^{13}C-labeled BPE, Ni/γ-Al_2O_3 (2 wt% Ni), and solvent 2-PrOH, pressurized with 121 bar H_2. In the ^{13}C spectra, all species are present as a pair of peaks, with the vapor phase at lower frequency than the liquid phase. The red and blue labels are defined in Scheme 3. (For interpretation of the references to colour in this figure legend, the reader is referred to the web version of this article.)
Adapted with permission [13]. Copyright 2018, American Chemical Society.

partial fellowship support.

This research is partially supported by the U.S. Department of Energy (DOE), Office of Basic Energy Sciences, Division of Chemical Sciences, Geosciences, and Biosciences. The Ames Laboratory is operated for the U.S. DOE by Iowa State University under Contract No. DE-AC02-07CH11358.

D.W.H. and E.D.W. acknowledge that portions of this rotor development were supported by the PNNL Laboratory Directed Research and Development program which includes technology maturation funds under projects 67228 and 68503. The high temperature/pressure solid-state NMR experiments were conducted at the Environmental Molecular Sciences Laboratory, a DOE Office of Science User Facility sponsored by the Office of Biological and Environmental Research. PNNL is operated by Battelle for the DOE under Contract DE-AC05-76RL01830.

References

[1] Zhang W, Xu S, Han X, Bao X. In situ solid-state NMR for heterogeneous catalysis: a joint experimental and theoretical approach. Chem Soc Rev 2012;41(1):192–210. https://doi.org/10.1039/C1CS15009J.

[2] Blasco T. Insights into reaction mechanisms in heterogeneous catalysis revealed by in situ NMR spectroscopy. Chem Soc Rev 2010;39(12). https://doi.org/10.1039/C0CS00033G. 4685-02.

[3] Yonker CR, Linehan JC. The use of supercritical fluids as solvents for NMR spectroscopy. Prog Nucl Magn Reson Spectrosc 2005;47(1):95–109. https://doi.org/10.1016/j.pnmrs.2005.08.002.

[4] Horváth IT, Millar JM. NMR under high gas pressure. Chem Rev 1991;91(7):1339–51. https://doi.org/10.1021/cr00007a003.

[5] Yonker CR, Zemanian TS, Wallen SL, Linehan JC, Franz JA. A new apparatus for the convenient measurement of NMR spectra in high-pressure liquids. J Magn Reson Ser A 1995;113(1):102–7. https://doi.org/10.1006/jmra.1995.1061.

[6] Wallen SL, Schoenbachler LK, Dawson ED, Blatchford MA. A polymer NMR cell for the study of high-pressure and supercritical fluid solutions. Anal Chem 2000;72(17):4230–4. https://doi.org/10.1021/ac0000630.

[7] Jonas J. High pressure NMR. Berlin, Heidelberg: Springer; 1991.

[8] Edwards T, Endo T, Walton JH, Sen S. Observation of the transition state for pressure-induced $BO_3 \rightarrow BO_4$ conversion in glass. Science 2014;345(6200):1027–9. https://doi.org/10.1126/science.1256224.

[9] Freude D, Hunger M, Pfeifer H. Study of brønsted acidity of zeolites using high-resolution proton magnetic resonance with magic-angle spinning. Chem Phys Lett 1982;91(4):307–10. https://doi.org/10.1016/0009-2614(82)80162-0.

[10] Munson EJ, Ferguson DB, Kheir AA, Haw JF. Applications of a new CAVERN design to the study of reactions on catalysts using in situ solid-state NMR. J Catal 1992;136(2):504–9. https://doi.org/10.1016/0021-9517(92)90080-2.

[11] Chen K, Abdolrhamani M, Sheets E, Freeman J, Ward G, White JL. Direct detection of multiple acidic proton sites in zeolite HZSM-5. J Am Chem Soc 2017;139(51):18698–704. https://doi.org/10.1021/jacs.7b10940.

[12] Hu JZ, Hu MY, Zhao Z, Xu S, Vjunov A, Shi H, et al. Sealed rotors for in situ high temperature high pressure MAS NMR. Chem Commun 2015;51(70):13458–61. https://doi.org/10.1039/C5CC03910J.

[13] Walter ED, Qi L, Chamas A, Mehta HS, Sears JA, Scott SL, et al. Operando MAS-NMR reaction studies at high temperatures and pressures. J Phys Chem C 2018;122(15):8209–15. https://doi.org/10.1021/acs.jpcc.7b11442.

[14] Prodinger S, Vjunov A, Hu JZ, Fulton JL, Camaioni DM, Derewinski MA, et al. Elementary steps of faujasite formation followed by in situ spectroscopy. Chem Mater 2018;30(3):888–97. https://doi.org/10.1021/acs.chemmater.7b04554.

[15] Zhao Z, Shi H, Wan C, Hu MY, Liu Y, Mei D, et al. Mechanism of phenol alkylation in zeolite H-BEA using in situ solid-state NMR spectroscopy. J Am Chem Soc 2017;139(27):9178–85. https://doi.org/10.1021/jacs.7b02153.

[16] Jung HB, Carroll K, Kabilan S, Heldebrant DJ, Hoyt D, Zhong L, et al. Stimuli-responsive/rheoreversible hydraulic fracturing fluids as a greener alternative to support geothermal and fossil energy production. Green Chem 2015;17(5):2799–812. https://doi.org/10.1039/C4GC01917B.

[17] Qi L, Alamillo R, Elliott WA, Andersen A, Hoyt DW, Walter ED, et al. Operando solid-state NMR observation of solvent-mediated adsorption-reaction of carbohydrates in zeolites. ACS Catal 2017:3489–500. https://doi.org/10.1021/acscatal.7b01045.

[18] Hu JZ, Sears JA, Mehta HS, Ford JJ, Kwak JH, Zhu K, et al. A large sample volume magic angle spinning nuclear magnetic resonance probe for in situ investigations with constant flow of reactants. Phys Chem Chem Phys 2012;14(7):2137–43. https://doi.org/10.1039/C1CP22692D.

[19] Hoyt DW, Turcu RVF, Sears JA, Rosso KM, Burton SD, Felmy AR, et al. High-pressure magic angle spinning nuclear magnetic resonance. J Magn Reson 2011;212(2):378–85. https://doi.org/10.1016/j.jmr.2011.07.019.

[20] Vjunov A, Hu MY, Feng J, Camaioni DM, Mei D, Hu JZ, et al. Following solid-acid-catalyzed reactions by MAS NMR spectroscopy in liquid phase—zeolite-catalyzed conversion of cyclohexanol in water. Angew Chem Int Ed 2014;53(2):479–82. https://doi.org/10.1002/anie.201306673.

[21] He T, Ren P, Liu X, Xu S, Han X, Bao X. Direct observation of DME carbonylation in the different channels of H-MOR zeolite by continuous-flow solid-state NMR spectroscopy. Chem Commun 2015;51(94):16868–70. https://doi.org/10.1039/C5CC07201H.

[22] Bowers GM, Schaef HT, Loring JS, Hoyt DW, Burton SD, Walter ED, et al. Role of cations in CO_2 adsorption, dynamics, and hydration in smectite clays under in situ supercritical CO_2 conditions. J Phys Chem C 2017;121(1):577–92. https://doi.org/10.1021/acs.jpcc.6b11542.

[23] Wilkins MJ, Hoyt DW, Marshall MJ, Alderson PA, Plymale AE, Markillie LM, et al. CO_2 exposure at pressure impacts metabolism and stress responses in the model sulfate-reducing bacterium *Desulfovibrio vulgaris* strain Hildenborough. Front Microbiol 2014;5. https://doi.org/10.3389/fmicb.2014.00507.

[24] Miller QRS, Thompson CJ, Loring JS, Windisch CF, Bowden ME, Hoyt DW, et al. Insights into silicate carbonation processes in water-bearing supercritical CO_2 fluids. Int J Greenhouse Gas Control 2013;15:104–18. https://doi.org/10.1016/j.ijggc.2013.02.005.

[25] Loring JS, Schaef HT, Turcu RVF, Thompson CJ, Miller QRS, Martin PF, et al. In situ molecular spectroscopic evidence for CO_2 intercalation into montmorillonite in supercritical carbon dioxide. Langmuir 2012;28(18):7125–8. https://doi.org/10.1021/la301136w.

[26] Bowers GM, Hoyt DW, Burton SD, Ferguson BO, Varga T, Kirkpatrick RJ. In situ ^{13}C and ^{23}Na magic angle spinning NMR investigation of supercritical CO_2 incorporation in smectite–natural organic matter composites. J Phys Chem C 2014;118(7):3564–73. https://doi.org/10.1021/jp410535d.

[27] Hoyt DW, Hu JZ, Sears JA, Walter ED, Mehta HS, Rosso KM, et al. Pressurized magic angle spinning (PMAS) technology for nuclear magnetic resonance (NMR) spectroscopy. R&D Magazine. 2015.

[28] Turcu RV, Hoyt DW, Rosso KM, Sears JA, Loring JS, Felmy AR, et al. Rotor design for high pressure magic angle spinning nuclear magnetic resonance. J Magn Reson 2013;226:64–9. https://doi.org/10.1016/j.jmr.2012.08.009.

[29] Bowers GM, Loring JS, Schaef HT, Walter ED, Burton SD, Hoyt DW, et al. Interaction of hydrocarbons with clays under reservoir conditions: in situ infrared and nuclear magnetic resonance spectroscopy and X-ray diffraction for expandable clays with variably wet supercritical methane. ACS Earth Space Chem 2018;2(7):640–52. https://doi.org/10.1021/acsearthspacechem.8b00039.

[30] Kwak JH, Hu JZ, Hoyt DW, Sears JA, Wang C, Rosso KM, et al. Metal carbonation of forsterite in supercritical CO_2 and H_2O using solid state ^{29}Si, ^{13}C NMR spectroscopy. J Phys Chem C 2010;114(9):4126–34. https://doi.org/10.1021/jp1001308.

[31] Kwak JH, Hu JZ, Turcu RV, Rosso KM, Ilton ES, Wang C, et al. The role of H_2O in the carbonation of forsterite in supercritical CO_2. Int J Greenhouse Gas Control 2011;5(4):1081–92. https://doi.org/10.1016/j.ijggc.2011.05.013.

[32] White MD, McGrail BP, Schaef HT, Hu JZ, Hoyt DW, Felmy AR, et al. Multiphase sequestration geochemistry: Model for mineral carbonation. Energy Procedia 2011;4:5009–16.

[33] Ok S, Hoyt DW, Andersen A, Sheets J, Welch SA, Cole DR, et al. Surface interactions and confinement of methane: a high pressure magic angle spinning NMR and computational chemistry study. Langmuir 2017;33(6):1359–67.

[34] Schaef HT, Loganathan N, Bowers GM, Kirkpatrick RJ, Yazaydin AO, Burton SD, et al. Tipping point for expansion of layered aluminosilicates in weakly polar solvents: supercritical CO_2. ACS Appl Mater Interfaces 2017;9(42):36783–91. https://doi.org/10.1021/acsami.7b10590.

[35] Loganathan N, Bowers GM, Yazaydin AO, Schaef HT, Loring JS, Kalinichev AG, et al. Clay swelling in dry supercritical carbon dioxide: effects of interlayer cations on the structure, dynamics, and energetics of CO_2 intercalation probed by XRD, NMR, and GCMD simulations. J Phys Chem C 2018;122(8):4391–402. https://doi.org/10.1021/acs.jpcc.7b12270.

[36] Morozova D, Wandrey M, Alawi M, Zimmer M, Vieth A, Zettlitzer M, et al. Monitoring of the microbial community composition in saline aquifers during CO_2 storage by fluorescence in situ hybridisation. Int J Greenhouse Gas Control 2009;4(6):981–9. https://doi.org/10.1016/j.ijggc.2009.11.014.

[37] Kothandaraman J, Dagle RA, Dagle VL, Davidson SD, Walter ED, Burton SD, Hoyt DW, Heldebrant DJ. Condensed phase low-temperature heterogeneous hydrogenation of CO2 to methanol. Catal. Sci. Technol. 2018;8:5098–103. https://doi.org/10.1039/C8CY00997J.